Journal of Positive Sciences (JPS) eISSN: 2582-9351, https://positive-sciences.com JPS. 2026 Jan; 6(2): 24-34

Article info
Received on: 05.01.2025
Accepted on: 11.02.2026
Published on: 13.02.2026
doi: https://doi.org/10.52688/ASP29096

Research Article

Enhancement of the biological properties of 316L stainless steel using chitosan-based biocomposite coatings via the sol–gel dip-coating technique

Omar Nadhom Qasim [1], Duaa S. Al-khafajy [2,*], Hanaa A. Al-Kaisy [3], Iman Adnan Annon [4], Mohammed RASHEED [5]

[1] Construction and Project Department, College of Engineering, University of Aliraqia, Baghdad 10066, Iraq
[2, 4, 5] College of Production Engineering and Metallurgy, University of Technology, Baghdad 10066, Iraq
[3] College of Materials Engineering, University of Technology, Baghdad 10066, Iraq

[*]Duaa.s.shams@uotechnology.edu.iq

ABSTRACT

The primary objective of this study is to enhance the biological performance of 316L stainless steel by applying biocomposite coatings derived from natural polymers. A chitosan/collagen blend was selected as the polymeric matrix due to its biocompatibility, biodegradability, and favorable bioactive properties. The coatings were fabricated using a sol–gel dip-coating technique, which enables controlled deposition, uniform thickness, and strong adhesion to the metallic substrate. To further improve functional performance, the matrix was reinforced with ceramic particles, namely titanium dioxide (TiO_2) and phosphorus pentoxide (P_2O_5), chosen for their bioactivity and antimicrobial potential. Structural characterization using X-ray diffraction (XRD) confirmed the crystalline phases of the incorporated ceramic reinforcements, verifying their successful integration into the polymer matrix. Field Emission Scanning Electron Microscopy (FESEM) analysis revealed smooth, homogeneous, and defect-minimized surfaces with a uniform dispersion of TiO_2 and P_2O_5 particles throughout the coating. Such morphology is essential for ensuring mechanical stability and long-term durability under physiological conditions. Surface energy and wettability measurements demonstrated that TiO_2-containing coatings exhibited lower contact angle values, indicating superior hydrophilicity compared to P_2O_5-reinforced layers. Enhanced wettability is associated with improved protein adsorption and cell attachment, which are critical factors for implant integration. Antibacterial assays further showed that TiO_2-modified surfaces exerted stronger inhibitory effects against both *Escherichia coli* and *Staphylococcus aureus*, suggesting effective resistance to bacterial colonization. These findings highlight that chitosan-based biocomposite coatings offer a promising and sustainable approach to improving the bioactivity, corrosion resistance, and antibacterial performance of stainless steel surgical implants.

Keywords: Stainless steel 316 L; biocomposite; coating; chitosan, sol-gel dip technique

INTRODUCTION

People who live longer have a higher chance of developing serious health problems such as bone damage and abnormalities (particularly beyond forty years of age). This increases the risk of long-term

*Corresponding author
Duaa S. Al-khafajy,
College of Production Engineering and Metallurgy, University of Technology, Baghdad 10066, Iraq
e-mail: Duaa.s.shams@uotechnology.edu.iq

musculoskeletal conditions such as osteoporosis, which is characterized by an increased risk of fractures, and osteoarthritis, which is a degenerative joint disease that can lead to a decline in mechanical properties, pain, and reduced functionality [1,2]. Therefore, biomaterials contribute to enhancing human lifespan and quality of life, and the biomaterials industry has grown rapidly to meet the needs of the aging population [3]. Metallic biomaterials are frequently used to repair arthritic or damaged joints, heal bone fractures, and stabilize and straighten the spinal column, such as Co–Cr alloys, titanium and its alloys, and stainless steel, which are non-biodegradable and remain as persistent foreign substances in the human body [4]. Due to their excellent corrosion resistance and biocompatibility, stainless steels are widely used biomaterials [5]. Without altering the bulk properties of the material, coating implants is considered a practical way to enhance implant–tissue interactions and promote biocompatibility and bifunctionality [6]. A coating is a protective layer applied to the metallic surface to minimize electrochemical reactions, provide long-term protection, and serve as a physical barrier between the material and its surroundings. The applied coatings must provide protection from damage, improve appearance, and offer additional functional properties [7]. In various industrial fields, dip-coating is a simple and cost-effective method for depositing coatings onto different substrates, such as fibers, ceramics, metals, and polymer films. The process involves applying liquid-phase coating solutions, often aqueous-based, onto the surface of a substrate. Typically, the material is immersed in the solution and then withdrawn to form a uniform coating layer [8]. Due to its inherent properties, including biodegradability, biocompatibility, anti-allergic characteristics, and biological activities (antibacterial, immune-enhancing, and antitumor effects), chitosan or its composites can be used to coat medical implants and create a bioactive surface [9,10]. Using bio-ceramic coatings is a practical way to improve corrosion resistance and biocompatibility, such as TiO_2, ZrO_2, and Nb_2O_5 [11]. In 2021, Rasha A. Issa et al. produced a thin coating layer using a polymer-based composite material (methyl methacrylate) reinforced with several bio-ceramics through the electrostatic deposition method. The findings showed that a uniform coating layer with excellent mechanical properties and no cracks was obtained [12]. In 2023, Maryam S. et al. studied the effect of TiO_2 nanotubes/CH-BG coatings applied to a titanium substrate following two-step surface treatments and showed that the surface hardness of the Ti substrate increased. In conclusion, the TNT/Chitosan-58S BG coating was found to be a suitable option for biomedical applications due to its favorable mechanical and electrochemical properties [13]. In 2022, QA Hamed et al. employed a dip-coating approach to apply biopolymer coatings made of chitosan and alginate with nanoparticles (TiO_2, Nb_2O_5) onto the surface of 316L stainless steel. According to FTIR and FESEM analyses, the coatings were homogeneous and free of cracks. The coated samples also exhibited notable hydrophilic properties. Furthermore, both particle-containing and non-particle-containing coatings demonstrated antibacterial activity [14].

The aim of this study is to evaluate the effect of chitosan-based biocomposite coatings reinforced with TiO_2 and P_2O_5 on the surface properties of 316L stainless steel, focusing on structural, morphological, wettability, and antibacterial characteristics.

EXPERIMENTAL WORK

MATERIAL REQUIRED

For sample preparation, 316L stainless steel was used as the substrate material. The samples were cut into dimensions of 2 cm × 2 cm × 1 mm. A belt grinder was utilized for the initial surface preparation. The surfaces were then polished sequentially using silicon carbide (SiC) abrasive papers with grit sizes of 100, 400, and 600 to obtain a smooth and uniform finish. After polishing, the samples were thoroughly cleaned with distilled water followed by ethanol to remove any surface contaminants. Finally, the specimens were dried in air at room temperature before coating.

For solution preparation, acetic acid diluted with distilled water was used as the solvent system. The polymers selected for the matrix were chitosan and collagen due to their biocompatibility and bioactive properties. Ceramic reinforcement particles, namely phosphorus pentoxide (P_2O_5) and titanium dioxide (TiO_2), were incorporated into the polymeric solution. A magnetic stirrer was used to ensure proper

*Corresponding author
Duaa S. Al-khafajy,
College of Production Engineering and Metallurgy, University of Technology, Baghdad 10066, Iraq
e-mail: Duaa.s.shams@uotechnology.edu.iq

dissolution of the polymers and uniform dispersion of the ceramic particles within the solution prior to the coating process.

COATING POWDER PREPARATION

To prepare the coating solution, chitosan powder was first dissolved in 4 mL of diluted acetic acid to obtain a milky and homogeneous solution. The solution was then placed on a magnetic stirrer to ensure complete dissolution and eliminate any entrapped air bubbles. The pH of the prepared solution was measured, and a NaOH solution was added dropwise to adjust the pH to 2.6. Separately, collagen was dissolved in 20 mL of distilled water until a clear solution was obtained. The prepared chitosan and collagen solutions were then mixed at a ratio of 1:1 (wt.%). The blended solution was magnetically stirred for one hour at room temperature at a rotational speed of 350 rpm to ensure proper mixing and uniformity. After achieving a homogeneous polymer matrix, ceramic reinforcements (P_2O_5 and TiO_2) were incorporated into the natural polymer matrix according to the compositions listed in Table 1. The composite coating layers were then deposited onto the 316L stainless steel substrates using the dip-coating technique.

Table 1: Composition of Coatings Deposited on 316L Stainless Steel Substrate.

Sample No.	Coating Composition (wt.%)
1	Matrix (Chitosan/Collagen)
2	15% P_2O_5 +85% matrix
3	15% TiO_2+85% matrix

RESULTS DISCUSSION

X-RAY DIFFRACTION

The XRD patterns of P_2O_5 and TiO_2 powders were recorded over a 2θ range and are presented in Fig. 1 and Fig. 2, respectively. The observed diffraction peaks were indexed to their corresponding lattice planes in accordance with the standard JCPDS card (No. 87-0952). The results confirm the crystalline nature of the starting ceramic powders used in the composite coatings [15]. Fig. 3 shows the XRD pattern of the composite coating reinforced with phosphorus pentoxide (P_2O_5). The diffractogram reveals the presence of highly intense and well-defined peaks, indicating the successful incorporation of P_2O_5 into the polymer matrix [16]. The characteristic peaks observed at 2θ values of approximately 20°, 22°, 26°, and 36° correspond to the crystalline phases of P_2O_5 within the composite coating [17]. Similarly, the XRD pattern of the chitosan/collagen-based composite coating reinforced with TiO_2 particles is presented in Fig. 4 [18]. The diffraction peaks located at 2θ values of approximately 20°, 22°, 25°, 37°, and 47° confirm the presence of TiO_2 within the coating [19-22]. All detected peaks are consistent with the characteristic reflections of TiO_2 in the anatase phase, as referenced by JCPDS card No. 73-1764. The peaks were well indexed to the corresponding tetragonal crystal structure, confirming the phase purity and successful reinforcement of TiO_2 in the biocomposite coating [23-27].

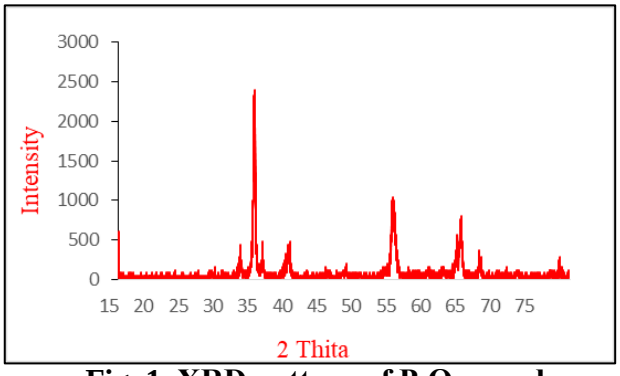

Fig. 1. XRD pattern of P_2O_5 powder

*Corresponding author
Duaa S. Al-khafajy,
College of Production Engineering and Metallurgy, University of Technology, Baghdad 10066, Iraq
e-mail: Duaa.s.shams@uotechnology.edu.iq

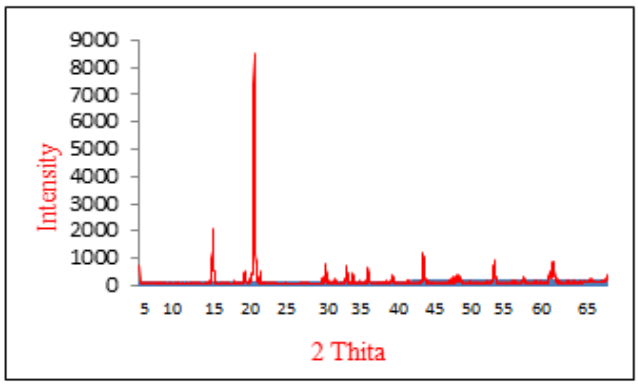

Fig. 2. XRD pattern of TiO_2 powder

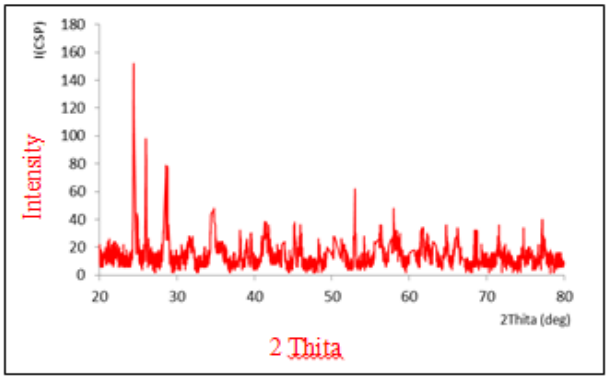

Fig. 3. XRD pattern of the natural polymer–based composite coating reinforced with P_2O_5 powder.

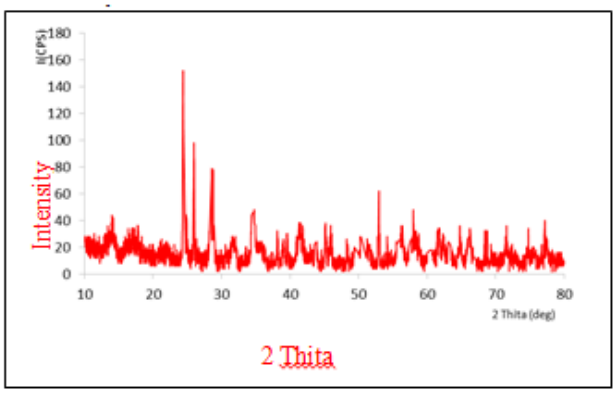

Fig. 4. XRD pattern of the natural polymer–based composite coating reinforced with TiO_2 powder

CONTACT ANGLE RESULT

The contact angle measurements obtained for all coated specimens (composite and hybrid coatings) after placing a water droplet on the surface for 30 seconds are presented in Fig. 5. The results indicate that all coated surfaces exhibited initial contact angle values below 90°, confirming their hydrophilic nature [28-30]. After droplet deposition, the water gradually spread and was almost completely absorbed, demonstrating excellent wettability of the coating layers. The metal substrate coated with the natural polymer matrix showed contact angle values of approximately 89° and 58°, indicating moderate hydrophilicity. In contrast, composite coatings reinforced with titanium dioxide (TiO_2) and phosphorus pentoxide (P_2O_5) exhibited lower contact angle values [31]. The decrease in contact angle became more

*Corresponding author
Duaa S. Al-khafajy,
College of Production Engineering and Metallurgy, University of Technology, Baghdad 10066, Iraq
e-mail: Duaa.s.shams@uotechnology.edu.iq

pronounced with the incorporation of ceramic particles, resulting in improved droplet spreading and absorption. Among the composite coatings, the TiO_2-reinforced specimen demonstrated the lowest contact angle (51.96°), indicating superior wettability compared to the P_2O_5-reinforced coating (62.11°), as shown in Fig. 6. The enhanced hydrophilicity of the ceramic-containing coatings can be attributed to the presence of surface particles, which increase surface energy and reduce the contact angle. Overall, the addition of ceramic reinforcements significantly improved the wettability of the composite coating materials, particularly in the case of TiO_2-based coatings [32].

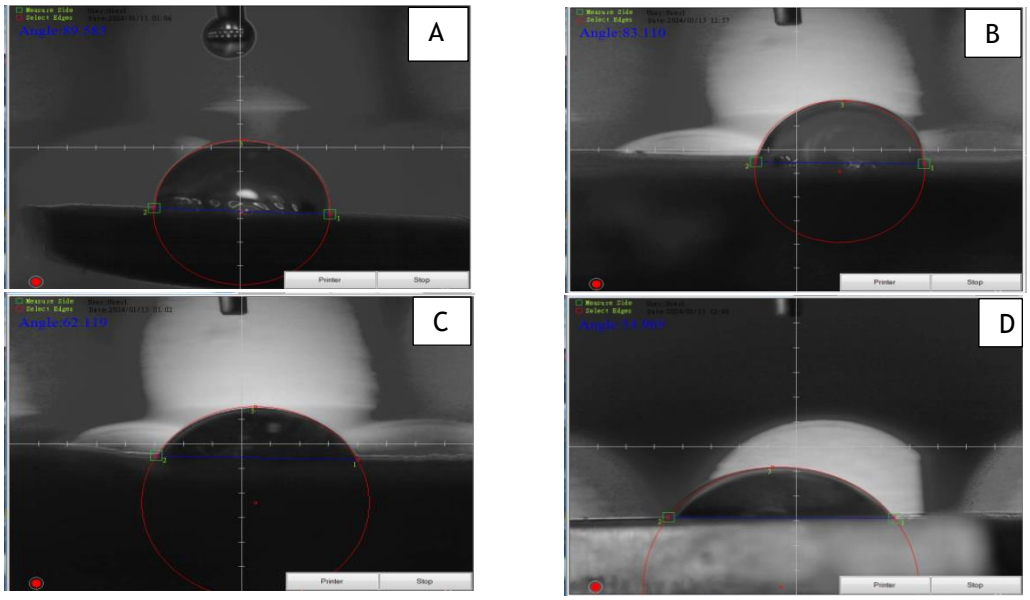

Fig. 5. Contact angle measurements of composite coatings after 30 seconds of water droplet deposition.

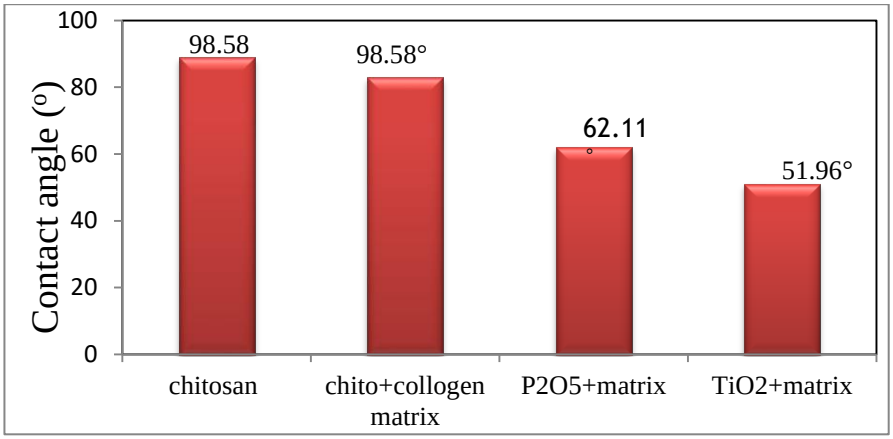

Fig. 6. Contact angle values of the composite coatings.

ANTIBACTERIAL ACTIVITY

The inhibition zones produced by the different coatings—P_2O_5- and TiO_2-reinforced (chitosan + collagen) composites—are presented in Figure 7, demonstrating their ability to suppress bacterial growth. Generally, a larger inhibition zone diameter indicates greater antibacterial effectiveness [33]. The size of the inhibition zone is directly associated with the level of antibacterial activity exhibited by the tested sample. Figure 8 shows that the composite coatings significantly inhibited bacterial growth, whereas the pure polymer matrix coating exhibited minimal or no antibacterial effect. It was also observed that the antibacterial activity decreased with increasing P_2O_5 content. Furthermore, the composite coatings containing P_2O_5 and TiO_2 within the chitosan + collagen matrix demonstrated stronger antibacterial activity against Escherichia coli compared to *Staphylococcus aureus (S. aureus)*. Both groups of reinforced coatings

*Corresponding author
Duaa S. Al-khafajy,
College of Production Engineering and Metallurgy, University of Technology, Baghdad 10066, Iraq
e-mail: Duaa.s.shams@uotechnology.edu.iq

exhibited clear and measurable zones of bacterial growth inhibition, confirming their promising antibacterial performance. These findings support the potential application of such biocomposite coatings as protective surface layers for biomedical implants, where reducing bacterial colonization is essential to minimize post-surgical infections [34, 35].

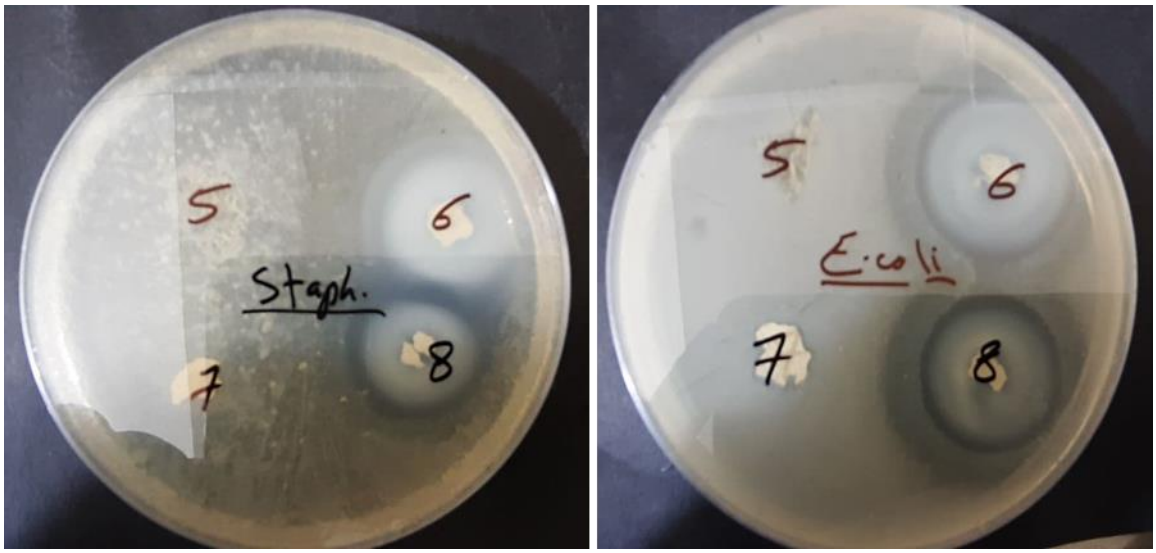

Fig. 7. Dimensions of the inhibition zones observed for the various samples on agar plates.

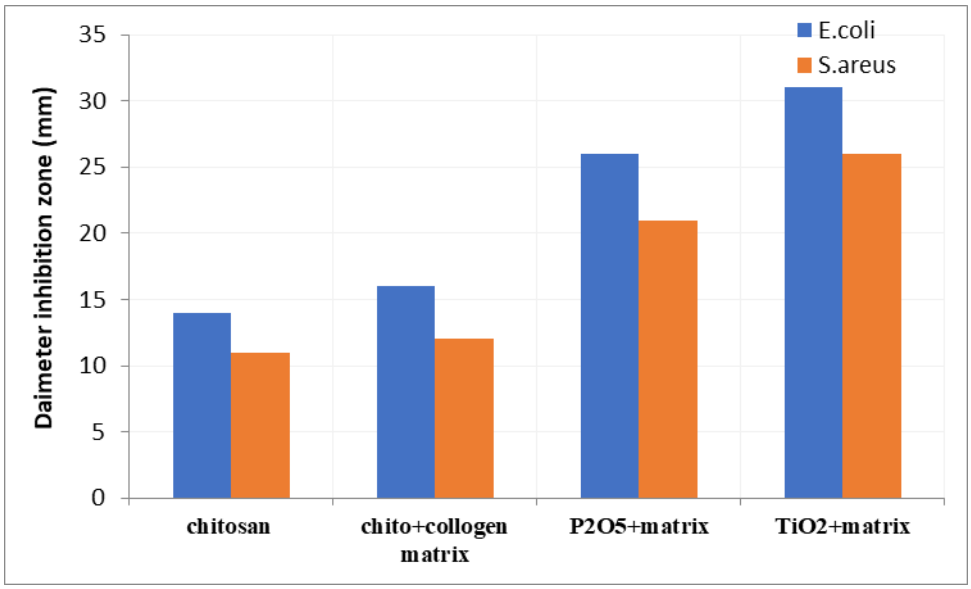

Fig. 8. Diameter of the inhibition zones for the various composite coating samples.

MORPHOLOGICAL ANALYSIS (FESEM)

The FESEM images of the chitosan/collagen coating and the composite coatings reinforced with P_2O_5 and TiO_2, prepared using the sol–gel dip-coating technique, are presented in Fig. 9. A homogeneous and porous film, characteristic of a polymeric matrix, was observed in the pure chitosan/collagen coating [36-38]. The micrographs revealed uniform coating deposition, along with consistent integration and distribution of ceramic particles throughout the chitosan/collagen matrix. Notably, no significant cracks or large pores were detected in the composite coatings. Such structural integrity is advantageous for biomedical applications, as it enhances mechanical stability and supports osseointegration. A continuous and uniform natural polymer layer covering the entire substrate surface can be clearly seen in Fig. 9 (b–d). The morphology of the deposited layer changed noticeably after the incorporation of P_2O_5 and TiO_2 compared to

*Corresponding author
Duaa S. Al-khafajy,
College of Production Engineering and Metallurgy, University of Technology, Baghdad 10066, Iraq
e-mail: Duaa.s.shams@uotechnology.edu.iq

the pure polymer coating. The addition of ceramic particles to the natural polymer matrix led to the formation of microscopic globular features on the surface, increasing surface roughness. This increased roughness is beneficial for improving cell attachment and biological interaction, thereby enhancing the overall bioactivity of the coating [39-41].

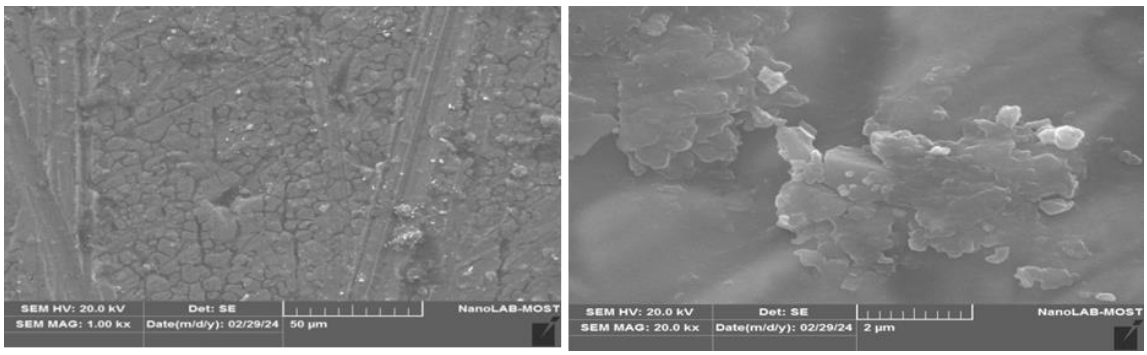

A) Chitosan

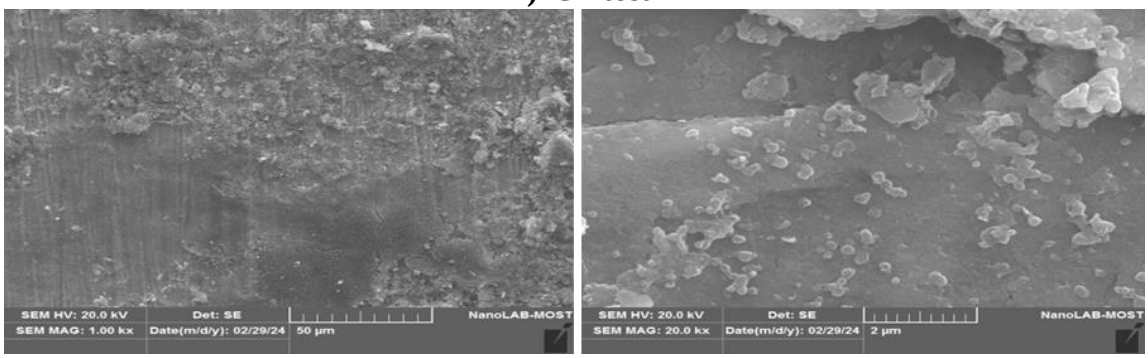

B) Chitosan+ collagen matrix

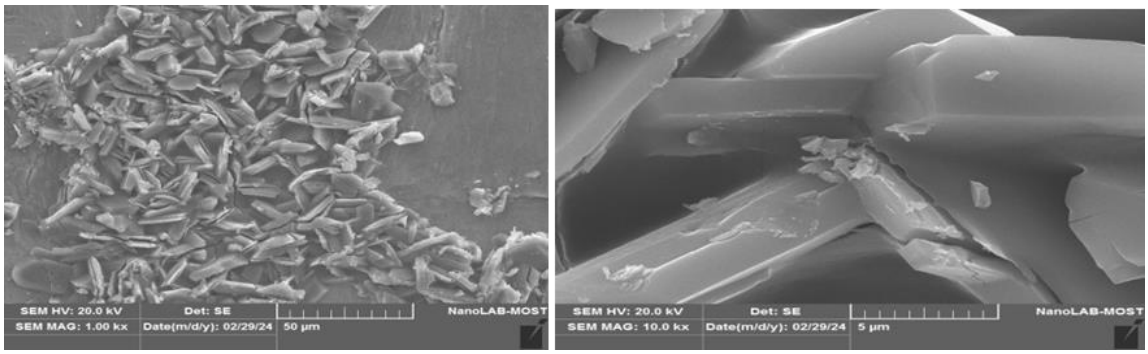

C) P_2O_5 + collagen matrix

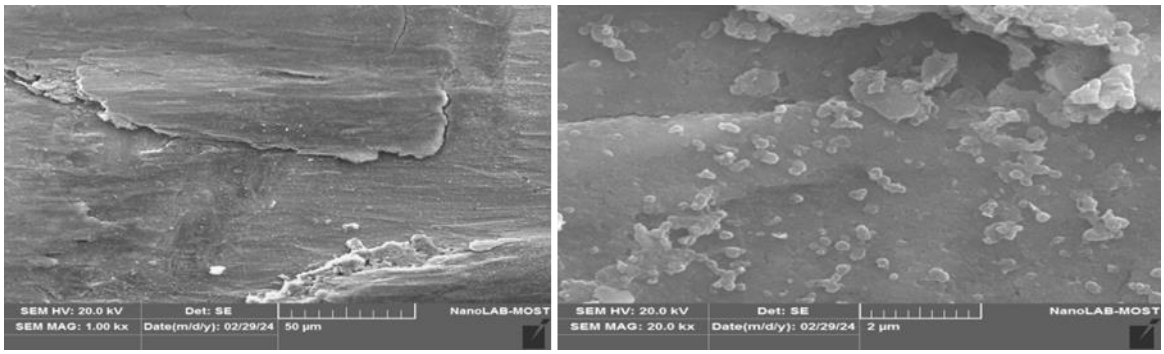

D) TiO_2 + matrix

Fig. 9. FESEM image of a) chitosan, b) chitosan+ collagen, c) P_2O_5 matrix and d) TiO_2 + matrix.

*Corresponding author
Duaa S. Al-khafajy,
College of Production Engineering and Metallurgy, University of Technology, Baghdad 10066, Iraq
e-mail: Duaa.s.shams@uotechnology.edu.iq

FOURIER-TRANSFORM INFRARED SPECTROSCOPY

Fourier Transform Infrared (FTIR) spectroscopy was used to characterize the coating materials and identify the organic and inorganic functional groups present on their surfaces. The FTIR spectrum of pure chitosan (Fig. 10a) shows characteristic absorption bands at 3352 cm^{-1} and 2852 cm^{-1}, which are attributed to the stretching vibrations of –OH and $–CH_3$ groups, respectively. Bands observed at 1598 cm^{-1} and 1435 cm^{-1} correspond to the bending vibration of the N–H group and the –OH vibration of the primary alcoholic group [42-44]. The peaks at 1382 cm^{-1} and 1061 cm^{-1} are assigned to C–O–N and C–O stretching vibrations, respectively, while the bands at 1144 cm^{-1} and 860 cm^{-1} are related to glycosidic linkages [15]. The FTIR spectrum of the chitosan–collagen natural polymer matrix (Fig. 10b) exhibited absorption bands at 2949, 2845, and 2990 cm^{-1}, corresponding to C–H stretching vibrations. The N–H stretching band around 2969 cm^{-1} showed a slight shift, indicating interactions between chitosan and collagen. The amide I and amide II bands appeared near 1640 cm^{-1} and 1547 cm^{-1}, respectively, with slight shifts in peak positions, suggesting hydrogen bonding and intermolecular interactions. Peaks observed at 1746 cm^{-1}, 1649 cm^{-1}, and 1447 cm^{-1} are attributed to the C=O groups, possibly associated with residual acetic acid and collagen functional groups. The C–H bending vibrations appeared at 911 cm^{-1} and 833 cm^{-1}. Overall, both coating groups exhibited similar FTIR spectral features. For the composite coating containing P_2O_5 (Fig. 10c), characteristic phosphate-related absorption bands were observed at 669–665 cm^{-1}, corresponding to PO_4 bending vibrations. Additional peaks at 1456–1375 cm^{-1} (PO_2 asymmetric stretching) and at 1061–1018 cm^{-1}, 992 cm^{-1}, and 839 cm^{-1} were assigned to P–O–P linkages in pyrophosphate groups and asymmetric stretching of non-bridging oxygen atoms bonded to phosphate units. Similar vibrational modes were detected in the TiO_2-reinforced coatings (Fig. 10d), with slight variations attributed to differences in ceramic particle concentration. The absence of new unexpected peaks indicates that no undesirable chemical reactions occurred between the composite components. This suggests good miscibility between the polymer matrix and ceramic reinforcements, as well as the absence of harmful by-products that could cause toxic or allergic effects in biomedical applications [45, 46].

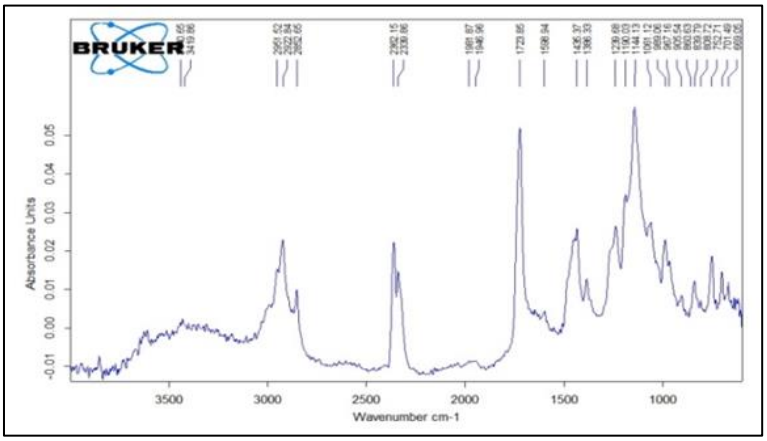

(a) Chitosan

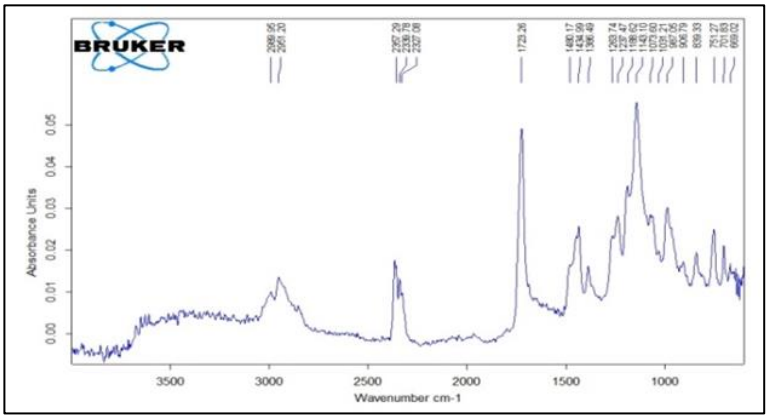

(b) Chitosan +collagen

*Corresponding author
Duaa S. Al-khafajy,
College of Production Engineering and Metallurgy, University of Technology, Baghdad 10066, Iraq
e-mail: Duaa.s.shams@uotechnology.edu.iq

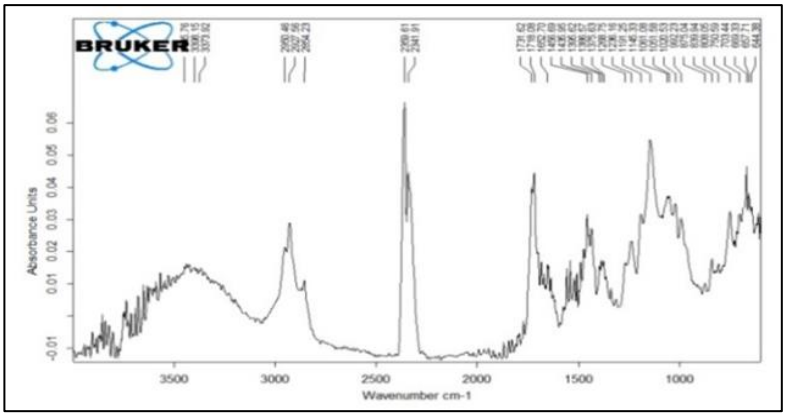

(c) Matrix

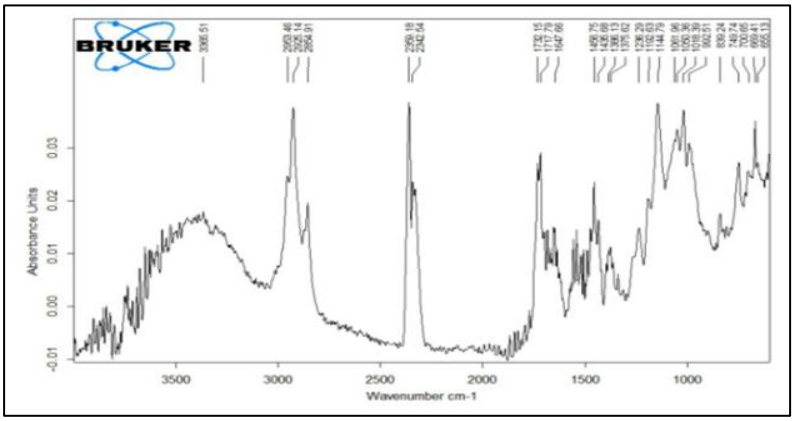

(d) Matrix + TiO_2

Fig. 10. FTIR spectrum of chitosan-PMMA/ P_2O_5 or TiO_2 coatings

CONCLUSION

The present study successfully demonstrates the fabrication of biocomposite coatings based on chitosan incorporated with ceramic reinforcements (TiO_2 and P_2O_5) on 316L stainless steel substrates using the sol–gel dip-coating technique. The selected method enabled the formation of uniform and adherent coatings with controlled thickness, highlighting its suitability for biomedical surface modification. X-ray diffraction (XRD) analysis confirmed the presence of crystalline phases within the coated layers, verifying the successful incorporation of ceramic constituents into the chitosan matrix without compromising structural integrity. Field emission scanning electron microscopy (FESEM) micrographs revealed homogeneous, dense, and crack-free surface morphologies, with ceramic particles uniformly distributed throughout the polymeric matrix. Such microstructural characteristics are critical for ensuring mechanical stability and long-term performance under physiological conditions. Wettability measurements showed a significant reduction in contact angle values, indicating enhanced surface hydrophilicity. Notably, TiO_2-reinforced coatings exhibited superior hydrophilic behavior, which is known to promote protein adsorption and cellular attachment—key factors for improved osseointegration. Furthermore, antibacterial assessments demonstrated a marked reduction in bacterial adhesion on coated samples compared to uncoated 316L stainless steel. The enhanced antibacterial performance, particularly in TiO_2-containing coatings, can be attributed to improved surface energy and possible photocatalytic or reactive oxygen species-related effects. Overall, the findings confirm that chitosan-based biocomposite coatings effectively enhance surface bioactivity, wettability, and antibacterial properties. These improvements significantly increase the potential of metallic implants for biomedical applications by promoting better tissue integration while minimizing the risk of post-implantation infections.

*Corresponding author
Duaa S. Al-khafajy,
College of Production Engineering and Metallurgy, University of Technology, Baghdad 10066, Iraq
e-mail: Duaa.s.shams@uotechnology.edu.iq

REFERENCES

[1] C. Prakash, H.K. Kansai, B.S. Pabla, S,Puri and A,Aggarwal, Electric discharge machining–A potential choice for surface modification of metallic implants for orthopedic applications: A review. Proceedings of the Institution of Mechanical Engineers, Part B: Journal of Engineering Manufacture, 2016. 230(2): p. 331-353.
[2] A. Nouri, and C. Wen, Introduction to surface coating and modification for metallic biomaterials. Surface coating and modification of metallic biomaterials, 2015: p. 3-60.
[3] G. Santos, , The importance of metallic materials as biomaterials. Adv Tissue Eng Regen Med Open Access, 2017. 3(1): p. 300-302.
[4] A. Nouri, AR, Shirvan, Y,Li and C, Wen, Surface modification of additively manufactured metallic biomaterials with active antipathogenic properties. Smart Materials in Manufacturing, 2023. 1: p. 100001.
[5] V. Zatkalíková, J, Halanda, D, Vana, M, Uhricik, L, Markovicova, M, Strbak and L, Kucharikova , Corrosion resistance of AISI 316L stainless steel biomaterial after plasma immersion ion implantation of nitrogen. Materials, 2021. 14(22): p. 6790.
[6] S.A. Jabbara, , N.J. Abdulkadera, and P.S. Ahmedb, Applying Nanocomposite Coatings to Improve Orthopedic Alloys by Using Multiple Flame Spray. Engineering and Technology Journal, 2023. 41(06): p. 870-885.
[7] S.A. Naser, , R.A. Anaee, and H.A. Jaber, Deposition of GdSmTi Coating for Corrosion Control of in Bio-Field. Engineering and Technology Journal, 2023. 41(06): p. 836-844.
[8] X. Tang, and X. Yan, Dip-coating for fibrous materials: mechanism, methods and applications. Journal of Sol-Gel Science and Technology, 2017. 81: p. 378-404.
[9] W. Tang, j, wang, H, Hou, Y, Li, J, Wang, J, Fu, L, Lu, D, Gao, Z, Lio, F, Zhao, X, Gao and P, Ling, Application of chitosan and its derivatives in medical materials. International Journal of Biological Macromolecules, 2023. 240: p. 124398.
[10] Kamila Rawojć ,Ryszard Tadeusiewicz1 and Ewa Zych-Stodolak, 2025. "Advancements in Chitosan-Based Scaffolds for Chondrogenic Differentiation and Knee Cartilage Regeneration: Current Trends and Future Perspectives." International Journal of Biological Macromolecules, Vol. 258, Part 1, 128912.
[11] N. Duraipandy, K.M. Syamala, and N. Rajendran, Antibacterial effects, biocompatibility and electrochemical behavior of zinc incorporated niobium oxide coating on 316L SS for biomedical applications. Applied Surface Science, 2018. 427: p. 1166-1181.
[12] R.A. Issa, M.N. Al-Shroofy, and H.A. Al-Kaisy, Al2O3-TiO2-PMMA bio-composite coating via electrostatic spray technique. Engineering and Technology Journal, 2021. 39(3A): p. 504-511.
[13] M. SafaviPour, H, Mokhtari, M, Mahmoudi, S, Fanaee, Z, Ghasemi, M, Kharaziha and A, Ashrafi, TiO2 nanotube/chitosan-bioglass nanohybrid coating: fabrication and corrosion evaluation. Journal of Applied Electrochemistry, 2023. 53(1): p. 177-189.
[14] Q.A. Hamad, S.A. Abdulrahman, and R.A.-H. Issa, Investigation some characteristics of biocomposites coating for biomedical implants. Key Engineering Materials, 2022. 936: p. 3-11.
[15] Shishir R., Nasiruddin U., Ponnilavan V., Rama Krishna L., Rameshbabu N.,
[16] Development of corrosion-resistant and bioactive ceramic-polymer hybrid coating over Zn 1Mg biodegradable implant material,Surface and Coatings Technology,Volume 487, 2024, 131031.
[17] M. Rasheed, et al., J. Adv. Biotechnol. Exp. Ther. 6(2) (2023) 495. https://doi.org/10.5455/jabet.2023.d144
[18] M. Rasheed, I. Alshalal, A.A. Ashed, M.A. Sarhan, A.S. Jaber, Indones. J. Electr. Eng. Comput. Sci. 33(1) (2024) 653. https://doi.org/10.11591/ijeecs.v33.i1.pp653-660
[19] I.M. Mohammed, M. Rasheed, AIP Conf. Proc. 3321 (2025) 020026. https://doi.org/10.1063/5.0289719
[20] F. Boudou, A. Belakredar, A. Berkane, M. Rasheed, Not. Sci. Biol. 17(2) (2025) 12183. https://doi.org/10.55779/nsb17212183
[21] F. Boudou, et al., Not. Sci. Biol. 17(3) (2025) 12593. https://doi.org/10.55779/nsb17312593
[22] F. Boudou, A. Guendouzi, A. Belkredar, M. Rasheed, Not. Sci. Biol. 16(2) (2024) 13837.

*Corresponding author
Duaa S. Al-khafajy,
College of Production Engineering and Metallurgy, University of Technology, Baghdad 10066, Iraq
e-mail: Duaa.s.shams@uotechnology.edu.iq

https://doi.org/10.55779/nsb16211837
[23] R.S. Mahmood, et al., J. Mech. Behav. Mater. 34 (2025) 1-15. https://doi.org/10.1515/jmbm-2025-0040
[24] T. Rashid, M.M. Mokji, M. Rasheed, J. Mech. Behav. Mater. 34 (2025) 77. https://doi.org/10.1515/jmbm-2025-0074
[25] M. Rasheed, M. N. Mohammedali, F. A. Sadiq, M. A. Sarhan, T. Saidani. J. Optics (New Delhi. Print) (2024). https://doi.org/10.1007/s12596-024-01928-5
[26] A.J. Hussein, M.N. Al-Darraji, M. Rasheed, M.A. Sarhan, IOP Conf. Ser.: Earth Environ. Sci. 1262 (2023) 022007. https://doi.org/ 10.1088/1755-1315/1262/2/022007
[27] A.J. Hussein, M.N. Al-Darraji, M. Rasheed, M.A. Sarhan, IOP Conf. Ser.: Earth Environ. Sci. 1262 (2023) 022005. https://doi.org/10.1088/1755-1315/1262/2/022005
[28] T. Saidani, M. Rasheed, I. Alshalal, A.A. Rashed, M.A. Sarhan, R. Barillé, Res. Eng. Struct. Mater. 10 (2) (2024) 743-770. http://dx.doi.org/10.17515/resm2023.21ma0922rs
[29] D. Bouras, M. Rasheed, Opt. Quantum Electron. 54 (2022) 12. https://doi.org/10.1007/s11082-022-04161-1
[30] A. Zubaidi, L.M. Asaad, I. Alshalal, M. Rasheed, J. Mech. Behav. Mater. 32 (2023) 1. https://doi.org/10.1515/jmbm-2022-0302
[31] M. Rasheed *et al.*, J. Phys.: Conf. Ser. 1999(1) (2021) 012080. https://doi.org/10.1088/1742-6596/1999/1/012080
[32] M. Rasheed, M.N. Al-Darraji, S. Shihab, A. Rashid, T. Rashid, J. Phys.: Conf. Ser. 1963 (2021) 1 012059. https://doi.org/10.1088/1742-6596/1963/1/012059
[33] M. Enneffatia, M. Rasheed, B. Louati, K. Guidara, S. Shihab, R. Barillé, J. Phys.: Conf. Ser. 1795(1) (2021) 012050. https://doi.org/10.1088/1742-6596/1795/1/012050
[34] M. Rasheed, O.Y. Mohammed, S. Shihab, A. Al-Adili, J. Phys.: Conf. Ser. 1795 (2021) 012043. https://doi.org/10.1088/1742-6596/1795/1/012043
[35] A.H. Ali, A.S. Jaber, M.T. Yaseen, M. Rasheed, O. Bazighifan, T.A. Nofal, Complexity 2022 (2022) 1-9. https://doi.org/10.1155/2022/9367638
[36] A. Jaber, M. Ismael, T. Rashid, M. A. Sarhan, M. Rasheed, I. M. Sala. Eureka: Phys. Eng. 4 (2023) 29–39. https://doi.org/10.21303/2461-4262.2023.002770
[37] T. Rashid, M. M. Mokji, M. Rasheed. J. Optics (2024). https://doi.org/10.1007/s12596-024-02080-w
[38] H. K. Aity, E. Dhahri, M. Rasheed. Ceram. Int. 50 (2024) part B 54666-54687. https://doi.org/10.1016/j.ceramint.2024.10.324
[39] M. Rasheed, S. Shihab, O. Alabdali, A. Rashid, T. Rashid, J. Phys.: Conf. Ser. 1999 (2021) 1 012077. https://doi.org/10.1088/1742-6596/1999/1/012077
[40] M. Rasheed, M. Nuhad Al-Darraji, S. Shihab, A. Rashid, T. Rashid. J. Phys.: Conf. Ser. 1963 (2021) 1 012058. https://doi.org/10.1088/1742-6596/1963/1/012058
[41] A. Keziz, M. Heraiz, F. Sahnoune, M. Rasheed, Ceram. Int. 49 (2023) 20 32989-33003. https://doi.org/10.1016/j.ceramint.2023.07.275
[42] E. Kadri, K. Dhahri, R. Barillé, M. Rasheed. Phase Transitions 94 (2021) 2 65–76. https://doi.org/10.1080/01411594.2020.1832224
[43] R. Jalal, S. Shihab, M.A. Alhadi, M. Rasheed, J. Phys.: Conf. Ser. 1660 (2020) 1 012090. https://doi.org/10.1088/1742-6596/1660/1/012090
[44] S. Shihab, M. Rasheed, O. Alabdali, A.A. Abdulrahman, J. Phys.: Conf. Ser. 1879 (2021) 2 022120. https://doi.org/10.1088/1742-6596/1879/2/022120
[45] A. Keziz, M. Heraiz, M. RASHEED, A. Oueslati. Mater Chem. Phys. 325 (2024) 129757. https://doi.org/10.1016/j.matchemphys.2024.129757.
[46] D. Kherifi, A. Keziz, M. Rasheed, A. Oueslati. Ceram. Int. 50 part A (2024) 30175. https://doi.org/10.1016/j.ceramint.2024.05.317

*Corresponding author
Duaa S. Al-khafajy,
College of Production Engineering and Metallurgy, University of Technology, Baghdad 10066, Iraq
e-mail: Duaa.s.shams@uotechnology.edu.iq